A Data-Driven Approach to the Prediction of Spheroidal Graphite Cast Iron Yield Surface Probability Characteristics

Mariya Shapovalova(✉) and Oleksii Vodka

National Technical University "Kharkiv Polytechnic Institute",
2 Kyrpychova Street, Kharkiv 61002, Ukraine
MiShapovalova@gmail.com, oleksii.vodka@gmail.com

Abstract. This work is aimed at studying material with a heterogeneous microstructure. The probabilistic characteristics of the yield surface are investigated. Statistically equivalent internal material structures are generated using computer simulations. The design takes into account the different amounts of spheroidal graphite inclusions concentration in the ferrite material. The stress state is calculated by the finite element method based on plane models. A series of experiments is calculated for each variant of the concentration of inclusions. The yield surfaces are determined. Based on the collected data, a study of the probabilistic characteristics of a random function is carried out. The radius function acts as a random variable. The number of intersections of the line with the yield surfaces is analyzed. The radii are constructed from the origin for each rotation angle along the closed circle. The proposed scheme takes into account the different behavior of composite materials under tensile and compressive loads. The probabilistic characteristics of the investigated quantity give a vision of the material operation modes at various loads. Going beyond the plasticity surface indicates the possibility of a product transition into a plastic state.

Keywords: Microstructure · Finite element method · Material properties · Probability · Yield surface

1 Introduction

An analysis of the collected data is one of the modern approaches to increasing the competitiveness of production. Nowadays, a data-driven approach helps to reduce the cost of production, allows predicting and avoiding equipment failures, contributes to improving the quality of products and processes. Big data analysis allows to track defects, identify the causes of inconsistencies, and eliminate them. A data-driven approach found application in artificial intelligence, engineering [1, 2, 5–7, 13, 14], strategy, marketing [3], policy, medicine [4], etc. It helps scientifically make decisions. In this article, such an approach applies to the prediction of yield surface probability characteristics.

Investigation of the probabilistic characteristics of the anisotropic materials yield surface [8–12], makes it possible to describe the behavior of a structure under a complex stress state. Identified weak points in the structure helps to avoid breakdowns.

M. Nechyporuk et al. (Eds.): ICTM 2020, LNNS 188, pp. 565–576, 2021.
https://doi.org/10.1007/978-3-030-66717-7_48

Carrying out numerous experiments is an expensive and laborious process. Computer modeling for predicting material behavior is an alternative to such an approach.

2 Objectives

As the initial data in this work, the results of previous studies are taken [15–17]. It is assumed that the microstructure is simulated synthetically based on real images of the material. The elastic properties and stress state of the sample are modeled by the finite element method.

The main objective of this study is to predict of spheroidal graphite cast iron yield surface probability characteristics. This objective requires the completion of such tasks:

- to create an experimental set of yield surfaces to ensure the absence of plastic deformations;
- to evaluate the influence of the inclusions concentration on the yield stress state during the tension and compression loading;
- to calculate the probability of plastic strain occurrence.

3 Generation of the Statistically Equivalent Artificial Microstructure

Image processing and artificial microstructure generation of statistically equivalent material have been implemented in previous works [15–17]. According to the results obtained in the articles, the creation of an equivalent structure is possible by establishing the dependence between the size and concentration of inclusions. The information about the quantity and size of inclusions located on a plane is collecting by using computer vision technology. The mathematical expectation data $M[R]$ and the variance $D[R]$ of the radii inclusions dependence on the concentration have been obtained by (1):

$$M[R] = 18.308 \cdot (\psi - 0.048)^{0.123}\ ;\ \sqrt{D[R]} = 9.683 \cdot (\psi - 0.045)^{0.314}. \qquad (1)$$

The location is followed to a uniform distribution and the size of inclusions is followed to a normal distribution function of concentration. Concentration (ψ) is defined as the ratio of the area of the inclusion to the area of the sample, which varies in the range of [0.055…0.3].

The finite element model construction is based on the artificial generated geometric model of the spheroidal graphite cast iron microstructure. To create the mesh grid, a two-dimensional 8-node finite element with two degrees of freedom in each node is used [21]. For calculation, is assumed that the main matrix of the investigate sample is isotropic ferrite and the inclusions are an orthotropic graphite material. The corresponding materials properties and elastic constants are given in Table 1 and Table 2. Various material properties and their resistance to tension and compression are taken into account.

Table 1. Properties of ferrite material (matrix).

E, GPa	ν	Yield strength, MPa
180	0.35	196

Table 2. Properties of graphite material (inclusions).

c_{11}, c_{22}	c_{12}	c_{13}, c_{23}	c_{33}	c_{44}, c_{55}	c_{66}	Yield strength	
						Compress	Tensile
GPa						MPa	
1060	290	109	46.6	2.3	435	31.9	3.9

To construct the yield surface, the model is considered under different loadings. Some of the typical load cases are presented in Fig. 1. The corresponding stress state of the model is shown in Fig. 2.

The model is represented by a square plate with a side – l. The deformation is set equal to $\varepsilon_\rho = \Delta l/l = 10^{-5}$, then the displacement is calculated by (2):

$$\begin{aligned} U_x &= \varepsilon_\rho \cdot l \cdot \cos\Theta, \\ U_y &= \varepsilon_\rho \cdot l \cdot \sin\Theta, \end{aligned} \tag{2}$$

where U_x, U_y is the displacement along the corresponding axis, $\Theta = (0\ldots360)^\circ$ the angle changes in a range, with a step in 3.6°.

Computer simulation methods are used to calculate the yield surface in a multi-dimensional stress state. This approach uses the hypothesis of yield strength under difficult loading conditions [8–12, 18]. Finding the yield surface is based on the hypothesis of the maximum distortion energy theory (the Huber - Mises - Hencky hypothesis) [19–21]. According to it, plastic strains of a sample in a complex stress state occurs when the specific formation energy becomes equal to or exceeds the specific formation energy of the material under the action of a uniaxial stress state.

For the microstructure which is consists of two types of materials (ferrite and graphite), the maximum stresses for each phase are found. For graphite, the tensile and compressive strengths differ significantly, therefore, separately for each type of stress state, the ratios maximum stresses to the corresponding allowable tensile strength are found. The yield surface is determined by the ratio of the principal stresses to the safety factor. The graphite material has a different tensile and compressive strength, therefore the dependence of the yield strength is calculated according to (3). Using the Heaviside step function of the first invariant of the stress tensor σ_0 with a coefficient equal to $k = 1\ \mu\text{Pa}^{-1}$ (4) and substituting it into (3), the final expression type for finding the yield stress of graphite is obtained by (5).

$$\sigma_{yield}^{graphite}(\sigma_0) \cong H(\sigma_0) \cdot \left(\sigma_{yield}^{tens} - \sigma_{yield}^{comp}\right) + \sigma_{yield}^{comp}, \tag{3}$$

$$H(\sigma_0) = \frac{1}{2} \cdot (1 + th(k \cdot \sigma_0)), \tag{4}$$

$$\sigma_{yield}^{graphite}(\sigma_0) \cong \frac{1}{2} \cdot (1 + th(k \cdot \sigma_0)) \cdot \left(\sigma_{yield}^{tens} - \sigma_{yield}^{comp}\right) + \sigma_{yield}^{comp}, \tag{5}$$

The dependence of the yield strength from the principal stresses for ferrite and graphite materials are shown in Fig. 3.

The calculation results of 250 random typical implementations of the yield surface are presented graphically in Fig. 4. This figure also contains results for ψ = (0.055, 0.100, 0.300).

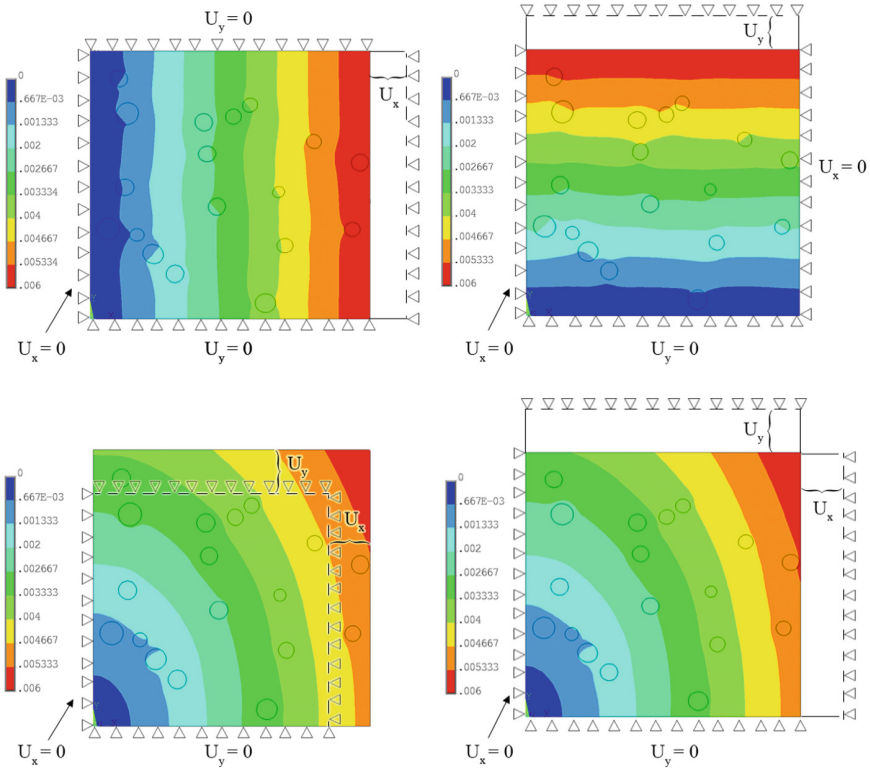

Fig. 1. Model displacement under different types of loads (ψ = 0.055).

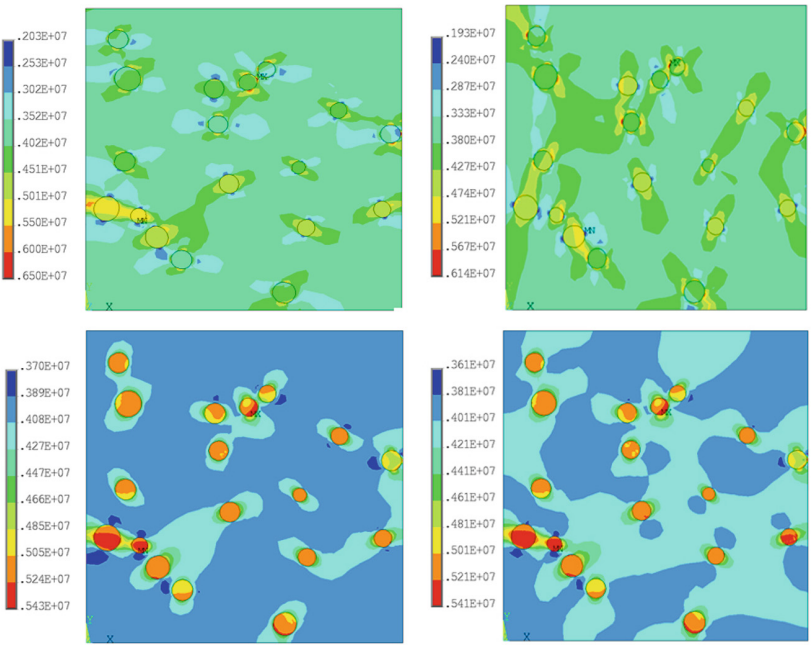

Fig. 2. Von Mises equivalent stresses under different types of loads ($\psi = 0.055$).

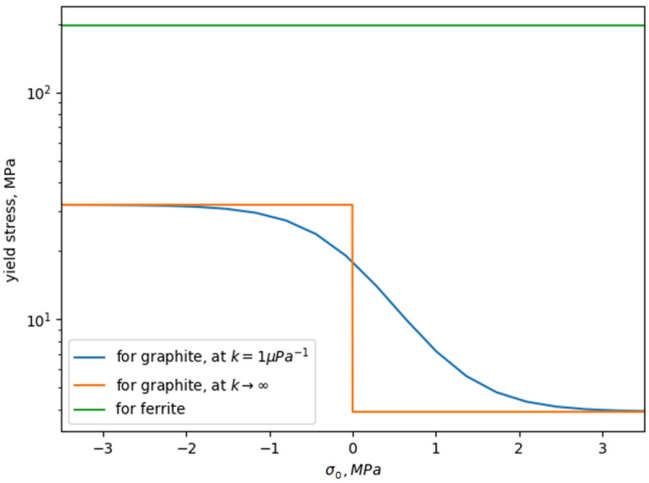

Fig. 3. The dependence of the yield strength from the principal stresses.

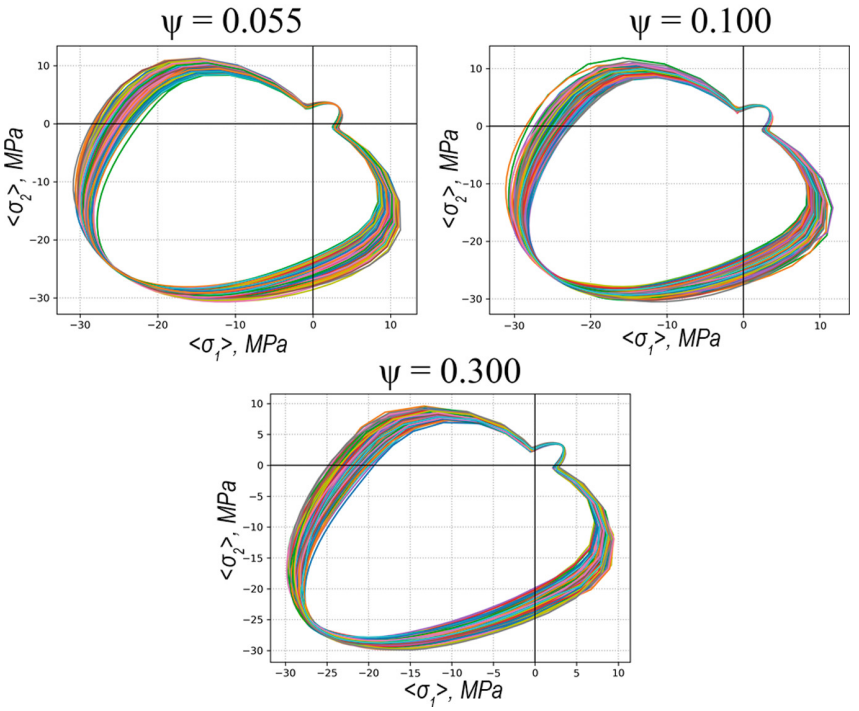

Fig. 4. Typical implementations of the yield surface arrangement.

4 Probability Estimation

The collected statistical data on the maximum allowable stresses for all components of the material under different types of loading leads to an assessment of the yield surface probabilistic characteristics.

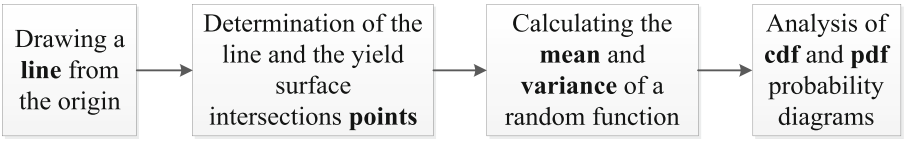

Fig. 5. Probability estimation schema.

A sequential diagram of the random variable estimation shown in Fig. 5. The accumulated statistical information on possible yield surface variants helps to determine the area of stress impact. In this work is using the construction of a line passing through the origin of the coordinates. Knowing the safe area of the stress, the measurement interval is set [1…40] MPa. The line intersects the graph of the yield surface is plotted point by point. The start point lies in the safe area, the endpoint is deliberately

chosen to lie outside the safe area. Along the line are selected 10000 control points. Some cases of the stress state in which the maximum allowable principal stresses for ferrite and graphite materials are located along the corresponding straight lines presented in Fig. 6.

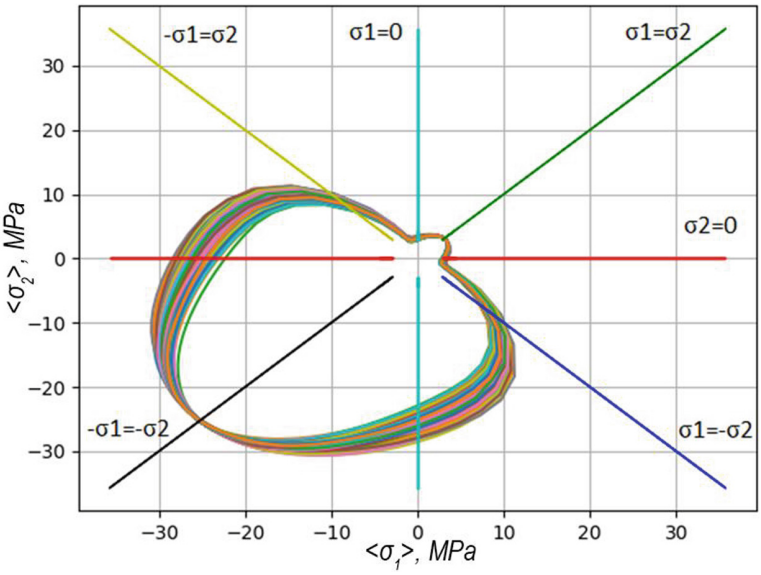

Fig. 6. Principal stresses location.

Information about the number of the yield surfaces that have fallen into the control points along the line are obtained. This method allowing to define the inverse cumulative distribution function $(1 - F(r))$, which in turn determining the parameters of descriptive statistics according to (6) and (7).

$$M[r] = \int_0^\infty (1 - F(r))dr, \tag{6}$$

$$\mathrm{var}[r] = \int_0^\infty 2r(1 - F(r))dr - M[r]^2, \tag{7}$$

where *M[r]* is the mathematical expectation (mean), and *var[r]* is the variance of the random radius function.

The corresponding distributions have been approximated by the normal law with the defined parameters. The dependence graph of the mean, standard deviation, and variation coefficient of the random radius function for the following concentrations of inclusions $\psi = (0.055, 0.100, 0.300)$, presented in Fig. 7. It can be seen that an increase

in the concentration of graphite inclusions leads to a decrease in the standard deviation, which, in turn, leads to an increase in the tensile strength of the material.

The coefficient of variation shows the extent of variability concerning the mean of the dataset. It's calculated as the ratio of the variance to the mathematical expectation. The obtained form of the coefficient of variation function corresponds to the different sample components material properties. The variance has the same tendency as the mean and depends proportionally.

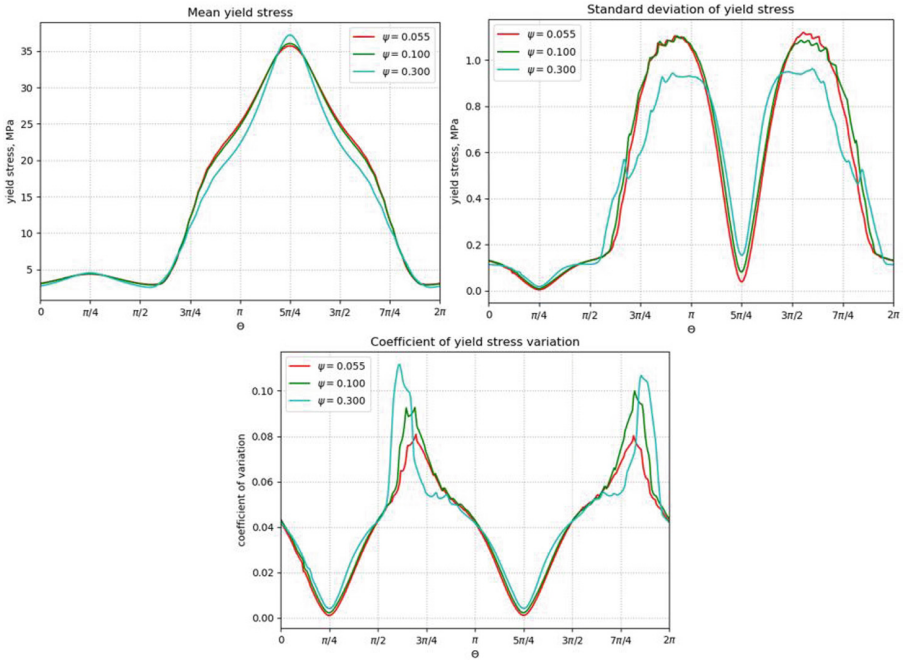

Fig. 7. Mean, standard deviation, and variation coefficient of the random radius function.

The reverse cumulative distribution functions of the yield surface intersection with a random function of the radii are shown in Fig. 8, and the probability distribution function is shown in Fig. 9. The analysis is carried out for several theta angles that correspond to the loading trajectory. The angles are calculated according to (8), and selected equal to Θ = (0, 45, 135, 300)°.

$$tg\Theta = \frac{\sigma_2}{\sigma_1}, \tag{8}$$

where σ_1 and σ_2 are the principal stresses.

Lines of different colors correspond to different angles, and the solid and dashed line styles correspond to calculated and fitted distribution function by **scipy.stats. norm.cdf** (Fig. 8). Results similar in values with insignificant deviation are obtained by graphic comparison of both methods.

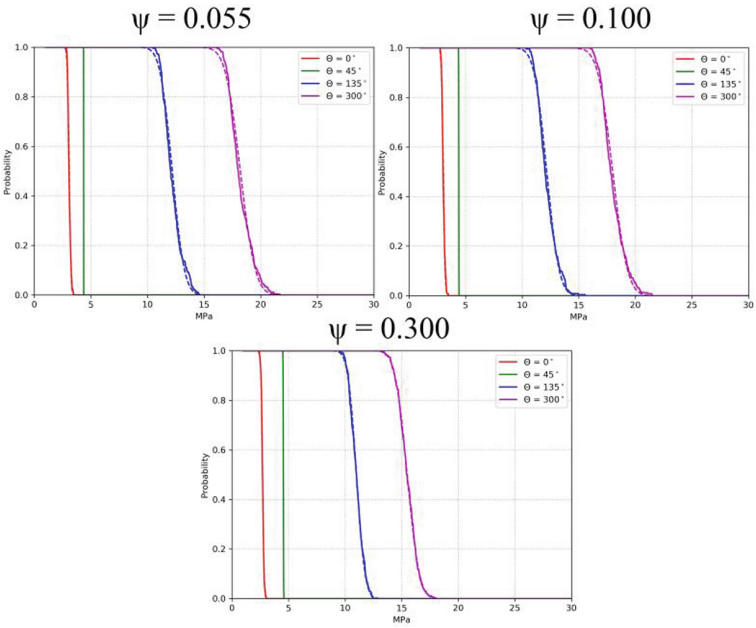

Fig. 8. Cumulative distribution function (cdf).

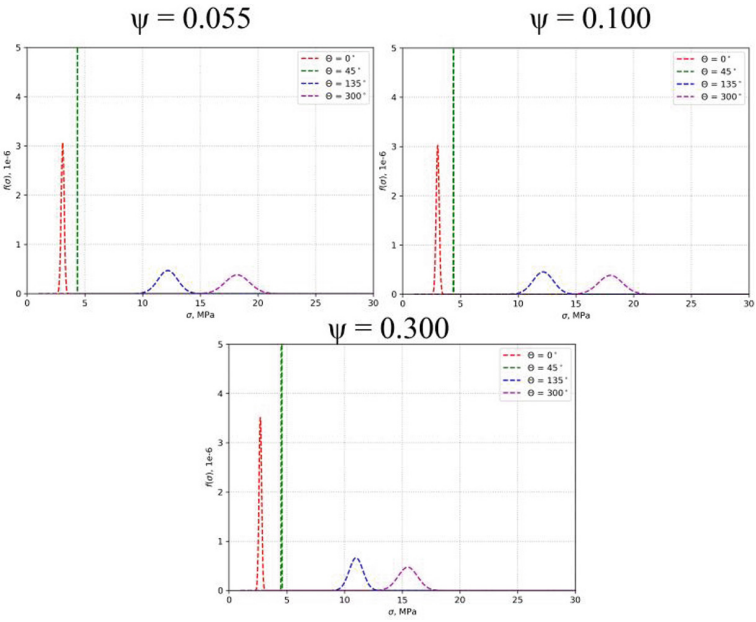

Fig. 9. Probability distribution function (pdf).

The dependence of the tensile and compression stress on the concentration of inclusions is shown in Fig. 10. The corresponding probabilistic characteristics at various concentrations of inclusions are given in Table 3.

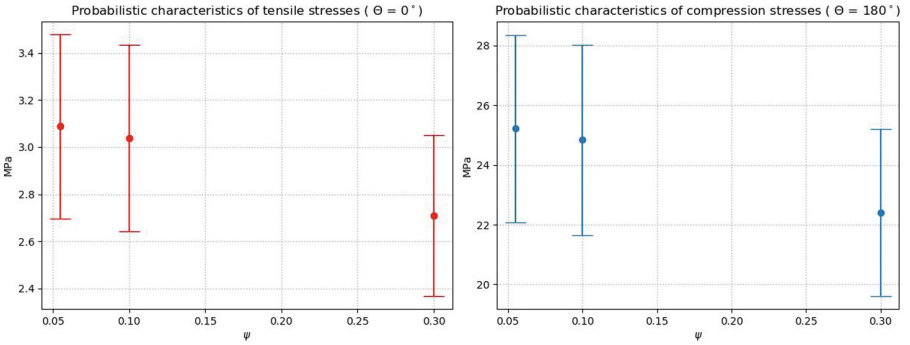

Fig. 10. Dependence of structural stress on the concentration of inclusions.

Table 3. Probabilistic characteristics of stresses at different concentration of inclusions.

Concentration, ψ	0.055	0.100	0.300
Tensile			
M, MPa	3.0879	3.0390	2.7103
$\sqrt{Var}$, MPa	0.1301	0.1320	0.1137
CV	0.0421	0.0434	0.0442
Compression			
M, MPa	25.224	24.840	22.403
$\sqrt{Var}$, MPa	1.0451	1.0598	0.9286
CV	0.0414	0.0427	0.0415

Analysis of the yield surface probabilistic characteristics shows the influence of the concentration of inclusions on the material strength characteristics. An increase in the concentration of graphite inclusions leads to the standard deviation decreases, which in turn of an increase in the material tensile strength. According to the results, the maximum spread of random typical implementations of the yield surface corresponds to the angle between stresses equal to $\Theta = 300°$, minimum – equal to $\Theta = 0°$. The spread in possible realizations of the yield surface is close to the minimum at equal values of the principal stresses ($\Theta = 45°$). The obtained standard deviation functions are not smooth (Fig. 7), which indicates a lack of statistical data and the need to expand the experimental base.

5 Conclusions

The article discusses an algorithm for studying of the yield surface probabilistic characteristics. The internal structure model is generated synthetically based on real material images. An experimental set of yield surfaces has been created. A method for determining the location of stresses and the yield surface is proposed. The probabilistic characteristics are calculated and the graphs of the distribution density are constructed. Going beyond the surface indicates the appearance of plastic strains in the model. The influence of the spheroidal graphite inclusions concentration in the ferrite composition is determined. With an increase in the concentration of inclusions in the model, a decrease in stresses and a decrease in their spread were noted both under compression and under tension.

According to 3-sigma rule, a spread for stress under tension $\sigma_{yield} = 3.0879 \pm 0.3904$ MPa for the smallest considered concentration ($\psi = 0.055$), which is decreases to $\sigma_{yield} = 2.7103 \pm 0.3411$ MPa for the greatest one ($\psi = 0.300$), the spread of the random variable is decreased too. For the stress under compression, a spread for stress take a form $\sigma_{yield} = 25.224 \pm 3.1352$ MPa for the smallest considered concentration ($\psi = 0.055$), which decreases to $\sigma_{yield} = 22.403 \pm 2.7858$ MPa for the greatest one ($\psi = 0.300$). The spread of the random variable is also decreased. It is also noted that the difference between the stress spread for the case of tension and compression differ by two orders of magnitude. Despite such a difference, the coefficient of variation for different concentrations and different types of loading is approximately the same (is equal to 0.0426 ± 0.0030).

Acknowledgment. This work has been supported by the Ministry of Education and Science of Ukraine in the framework of the realization of the research project «Development of methods for mathematical modeling of the behavior of new and composite materials aims to structural elements lifetime estimation and prediction of engineering designs reliability» (State Reg. Num. 0117U004969).

References

1. Lvov, G., Kostromytska, O.: A data-driven approach to the prediction of plasticity in composites. In: Nechyporuk, M., et al. (eds) Integrated Computer Technologies in Mechanical Engineering. AISC, vol. 1113, pp. 3–10. Springer, Cham (2020). https://doi.org/10.1007/978-3-030-37618-5_1
2. Amir Siddiq, M.: Data-driven finite element method: theory and applications. In: Proceedings of the Institution of Mechanical Engineers, Part C: Journal of Mechanical Engineering Science (2020). https://doi.org/10.1177/0954406220938805
3. Shah, D., Murthi, B.P.S.: Marketing in a data-driven digital world: implications for the role and scope of marketing. J. Bus. Res. (2020). https://doi.org/10.1016/j.jbusres.2020.06.062
4. Barmparis, G.D., Tsironis, G.P.: Estimating the infection horizon of COVID-19 in eight countries with a data-driven approach. Chaos Solitons Fractals **135**, 109842 (2020). https://doi.org/10.1016/j.chaos.2020.109842

5. Bessa, M., Bostanabad, R., Liu, Z., et al.: A framework for data-driven analysis of materials under uncertainty: countering the curse of dimensionality. Comput. Methods Appl. Mech. Eng. **320**, 633–667 (2017). https://doi.org/10.1016/j.cma.2017.03.037
6. Latypov, M.I., Kalidindi, S.R.: Data-driven reduced order models for effective yield strength and partitioning of strain in multiphase materials. J. Comput. Phys. **346**, 242–261 (2017). https://doi.org/10.1016/j.jcp.2017.06.013
7. Chan, K.S.: Effects of plastic anisotropy and yield surface shape on sheet metal stretchability. Metall. Trans. A **16**(4), 629 (1985). https://doi.org/10.1007/BF02814237
8. Wu, B., Wang, H., Taylor, T., Yanagimoto, J.: A non-associated constitutive model considering anisotropic hardening for orthotropic anisotropic materials in sheet metal forming. Int. J. Mech. Sci. **169**, 105320 (2020). https://doi.org/10.1016/j.ijmecsci.2019.105320
9. Lu, D., Zhang, K., Hu, G., et al.: Investigation of yield surfaces evolution for polycrystalline aluminum after pre-cyclic loading by experiment and crystal plasticity simulation. Materials **13**(14), 3069 (2020). https://doi.org/10.3390/ma13143069
10. Tang, S., Li, Y., Qiu, H., et al.: MAP123-EP: a mechanistic-based data-driven approach for numerical elastoplastic analysis. Comput. Methods Appl. Mech. Eng. **364**, 112955 (2020). https://doi.org/10.1016/j.cma.2020.112955
11. Zhang, H., Diehl, M., Roters, F., Raabe, D.: A virtual laboratory using high resolution crystal plasticity simulations to determine the initial yield surface for sheet metal forming operations. Int. J. Plast. **80**, 111–138 (2016). https://doi.org/10.1016/j.ijplas.2016.01.002
12. Banabic, D., Barlat, F., Cazacu, O., Kuwabara, T.: Advances in anisotropy and formability. Int. J. Mater. Form. **3**(3), 165–189 (2010). https://doi.org/10.1007/s12289-010-0992-9
13. Larin, A.A., Vyazovichenko, Y.A., Barkanov, E., Itskov, M.: Experimental investigation of viscoelastic characteristics of rubber-cord composites considering the process of their self-heating. Strength Mater. **50**(6), 841–851 (2018). https://doi.org/10.1007/s11223-019-00030-7
14. Larin, O., Potopalska, K., Mygushchenko, R.: Statistical estimation of residual strength and reliability of corroded pipeline elbow part based on a direct FE-simulations. J. Serb. Soc. Comput. Mech. **12**(1), 80–95 (2018). https://doi.org/10.24874/jsscm.2018.12.01.06
15. Shapovalova, M., Vodka, O.: Image microstructure estimation algorithm of heterogeneous materials for identification their chemical composition. In: 2019 IEEE 2nd Ukraine Conference on Electrical and Computer Engineering (UKRCON), pp. 975–979. IEEE, Lviv (2019). https://doi.org/10.1109/UKRCON.2019.8879861
16. Shapovalova, M., Vodka, O.: Computer methods for constructing parametric statistically equivalent models of high-strength cast iron microstructure to analyze its elastic characteristics. Notes of the V.I. Vernadsky Tavrida National University. Ser. Tech. Sci. **30**(6), 179–187 (2019). https://doi.org/10.32838/2663-5941/2019.6-1/33 [in Ukrainian]
17. Shapovalova, M., Vodka, O.: Computer methods for modeling the synthetic structure of cast iron for statistical evaluation of its mechanical properties and strength characteristics. Theoret. Appl. Mech. **35**, 257–264 (2020). [in Russian]
18. Annin, B., Ostrosablin, N.: Anisotropy of the elastic properties of materials. Appl. Mech. Tech. Phys. **49**(6), 131–151 (2008). [in Russian]
19. Beliaev, N.: Strength of Materials. Nauka, Moscow (1965). [in Russian]
20. Ambatsumian, S.: Theory of Anisotropic Plates. Nauka, Moscow (1967). [in Russian]
21. Zienkiewicz, O.: The Finite Element Method in Engineering Science. McGraw-Hill, London (1971)